

3.0 SOMBRERO KRF-LASER DRIVEN POWER PLANT

3.1 SUMMARY OF SOMBRERO PLANT PARAMETERS

SOMBRERO is a 1000 MWe, KrF-laser driven power plant design. The SOMBRERO chamber is constructed of a low-activation carbon/carbon (C/C) composite. The first wall is protected with 0.5 torr of xenon buffer gas. Solid Li_2O particles flow by gravity through the blanket as the primary coolant and breeding material. This moving bed solid breeder blanket design has all the advantages of solid breeders but none of the disadvantages, such as the need for a high pressure gas coolant and a separate He gas loop for tritium extraction. Previous flowing solid breeder designs include a tokamak,⁹ SOLASE,¹⁰ and Cascade.¹¹ Helium is used to fluidize the particles for transport around the heat transfer loop. Liquid lead is used in the intermediate loop to transfer heat to a steam generator and a double reheat steam power cycle.

The KrF driver uses e-beam pumped amplifiers and angular multiplexing for pulse compression. The laser uses relatively small (~60 kJ) final amplifiers and a new plasma cathode technology for the e-beams in order to improve the laser system efficiency. Amplifiers are grouped in four-unit modules to minimize hardware requirements. Sixty beams are used to provide uniform target illumination. Grazing incidence metal mirrors are used as the final optical component to remove the dielectric focusing mirrors from the direct line of sight of high energy neutrons.

The key plant operating parameters are listed in Table 3.1.

3.2 SOMBRERO CHAMBER DESIGN

A cross section of the SOMBRERO chamber is shown in Fig. 3.1, and the key design parameters are given in Table 3.2. The chamber is assembled from 12 wedge-shaped, carbon/carbon composite modules that are totally independent of each other with separate Li_2O inlet and outlet tubes. The chamber has a cylindrical central section with conical ends, a radius of 6.5 m at the midplane, and an overall height of 18 m. Each module is subdivided both radially and circumferentially into coolant channels as shown in Fig. 3.2. The carbon structure fraction increases from 3% at the front to 50% at the rear of the blanket, thus providing an integral reflector which does not require separate cooling. The first wall (FW) thickness is 1.0 cm. The thickness of the coolant channel behind the FW varies from 7 cm at the midplane to 37 cm at the upper and lower extremities, making the flow area constant along the entire FW from top to bottom. This is done to ensure a constant velocity at the FW where a high heat transfer coefficient is needed.

Table 3.1. SOMBRERO Power Plant Operating Parameters

Driver Energy (MJ)	3.4
Target Gain	118
Target Yield (MJ)	400
Rep Rate (Hz)	6.7
Fusion Power (MW)	2677
Energy Multiplication	1.08
Total Thermal Power (MW)	2891
Power Conversion Efficiency (%)	47
Gross Electrical Power (MWe)	1359
Driver Efficiency (%)	7.5
Driver Power (MWe)	304
Auxiliary Power (MWe)	55
Net Electric Power (MWe)	1000
Tritium Breeding Ratio	1.25

Table 3.2. SOMBRERO Chamber Design Parameters

First Wall Radius at Midplane (m)	6.5
Overall Internal Height (m)	18
First Wall Thickness (cm)	1.0
Maximum Stress in First Wall (MPa)	43
Blanket Thickness (m)	1.0
Total Thermal Power (MW)	2981
Surface Power (MW)	803
Blanket Power (MW)	2088
Li ₂ O Inlet Temperature (°C)	550
Li ₂ O Avg. Outlet Temperature (°C)	740
Li ₂ O Flow Rate (kg/s)	5590
Max Li ₂ O Velocity at FW (m/s)	1.15
Number of Blanket Modules	12
Structural Mass Per Module (Tonne)	37.8
Number of Beam Ports	60
Li ₂ O Mass in Chamber (kg)	670,000
Total Li ₂ O Inventory (kg)	2,000,000

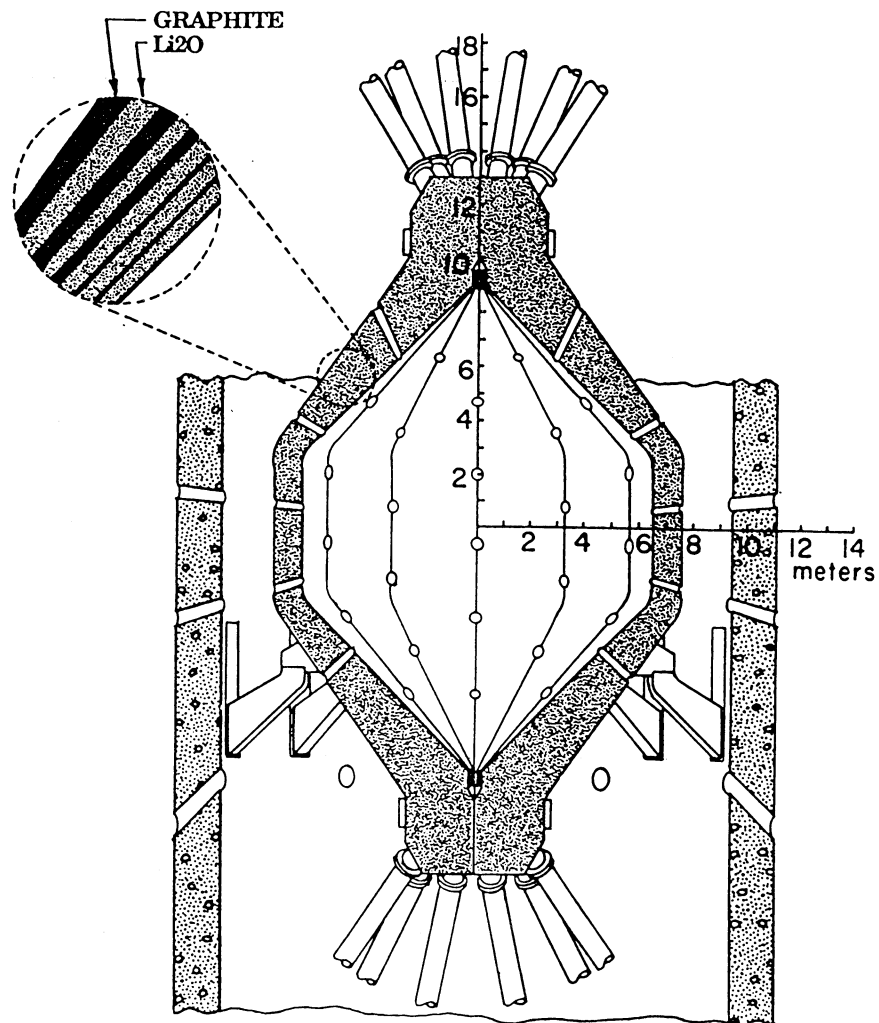


Fig. 3.1. Cross section of SOMBRERO Chamber.

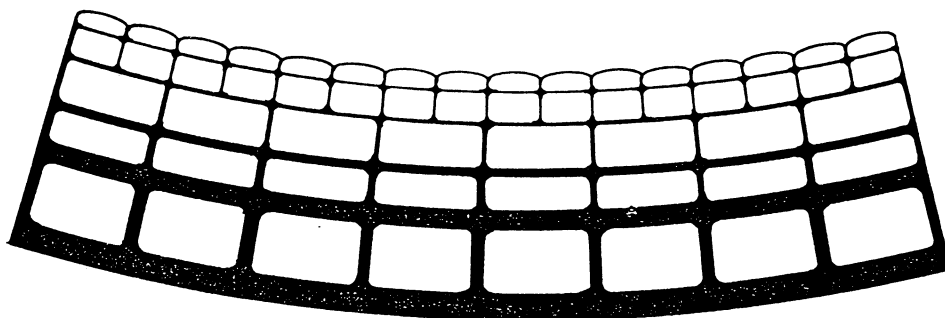


Fig. 3.2. Cross Section of SOMBRERO Blanket.

The Li_2O particles with a size range of 300-500 μm have a void fraction of 40% in the moving bed, and the grains are 90% of theoretical density. The Li_2O particles enter the top of the chamber from a manifold that doubles as a cyclone separator to remove the particles from the He gas that is used to transport Li_2O through the intermediate heat exchanger (IHX). After the particles enter the chamber, they flow under the force of gravity through the chamber and exit at the bottom. The Li_2O velocity at the FW is 1.15 m/s, and each succeeding radial zone has progressively lower velocities toward the rear of the blanket. Low pressure (0.2 MPa) He gas flows counter-current to the particles in the chamber coolant channels; this helps maintain a steady movement of the particles and prevents the formation of clustering or compaction. A thin coating of SiC on the inner surface of the coolant channels aids in sealing the C/C composite structure against He gas leakage into the chamber. The Li_2O inlet temperature to all the zones is 550°C, but the outlet temperature is 700°C for the FW coolant channel and 800°C for the rear zones. The total mass flow rate of 2×10^7 kg/hr has an equilibrated outlet temperature of 740°C. Flow in the different zones is controlled with baffles located at the bottom of the chamber to ensure that there will be no voids in the blanket. After going through the chamber, the particles are transported around the loop and through the IHX in a fluidized or entrained state by He gas.

The FW is protected from x-rays and ions by 0.5 torr of Xe gas. Since the beam ports are open to the reactor building, the whole building also has 0.5 torr of Xe gas. A certain amount of He leakage into the building can be tolerated without degrading the reactor performance. Innovative ideas for separating He from Xe, such as diffusion membranes, must be incorporated into the Xe recycling system.

SOMBRERO also has very good neutronic performance. The tritium breeding ratio is 1.25 with 0.91 coming from ${}^6\text{Li}$. The energy multiplication factor is 1.08, which increases the 2677 MW of fusion power to 2891 MW of total thermal power. The peak displacement damage rate in the carbon first wall is about 15 dpa/fpy, and the helium production rate is about 3800 appm/fpy. The lifetime limit for radiation damage is uncertain. We assume that a materials program can develop a C/C composite with a damage limit of 75 dpa, which would give a first wall lifetime of ~ 5 fpy.

3.3 SOMBRERO POWER CONVERSION AND PLANT FACILITIES

3.3.1 Heat Transport System

The primary coolant for SOMBRERO is a flowing bed of Li_2O particles in He gas and operates between 550 and 740°C. The primary loop consists of four coolant circuits including one IHX in each circuit. The number of circuits is based on the size of the heat exchangers. A state-of-the-art heat exchanger design is assumed. An intermediate loop, with lead coolant operating

between 400 and 600°C, is used to isolate the SOMBRERO chamber from the high pressure steam loop. The coolant parameters are the same as in the case of Osiris.

3.3.2 Power Conversion

To achieve a high efficiency power conversion, a high pressure, high temperature steam cycle, similar to the Osiris plant, was adopted for the SOMBRERO plant. The steam conditions are the same as for the Osiris plant, with a peak pressure of 24.2 MPa and peak temperature of 538°C. As previously noted, these conditions provide a thermal conversion efficiency of 45%. However, in the case of SOMBRERO, 230 MWt of laser waste heat is used for feedwater heating, and this increases the cycle efficiency to 47%.

There are two steam generators, and each is sized for 50% of the thermal capacity (1490 MWt). The steam generator arrangement is similar to that of the Osiris plant. Each steam generator is made up of three separate vessels: superheater, first reheater, and second reheater.

The reactor plant is provided with a turbine-generator capable of generating 1360 MWe gross electrical power. Each turbine-generator is a state-of-the-art design consisting of a high-pressure section, an intermediate-pressure section, and two low-pressure sections arranged in a cross-compound configuration.

3.3.3 Reactor Building

A concept for the SOMBRERO reactor building has been developed. The building provides housing for the reactor, shielding of the public from fusion neutrons, and housing for the final optics. In addition, the building accommodates remote maintenance of the reactor. The concept for this building is shown in Figs. 3.3 and 3.4.

The size of the reactor building is dictated by the requirements for housing the final optics of the laser driver. It accommodates 60 beam lines that offer a near-uniform illumination. All the beam lines penetrate the reactor building through a beam handling area in the basement. The building vacuum boundary is located at the building floor where the beam lines penetrate the floor through windows.

The layout of the final optics is determined by the requirement for reasonable lifetimes of the final optics, which is highly uncertain since there are almost no data on radiation damage of either metal or dielectric optics in high neutron fluences. Grazing incidence metal mirrors (GIMM) made of aluminum are used to bend the beams slightly (84° angle of incidence) so that the dielectric focusing mirrors are out of the direct line of sight of fusion neutrons. The GIMMs are located 30 m from the center of the chamber, and the dielectric focusing mirrors are 50 m from the center of the chamber. Neutron dumps are located behind the GIMMs to further reduce the neutron flux experienced by the dielectric optics, which are expected to survive for the life of the plant without

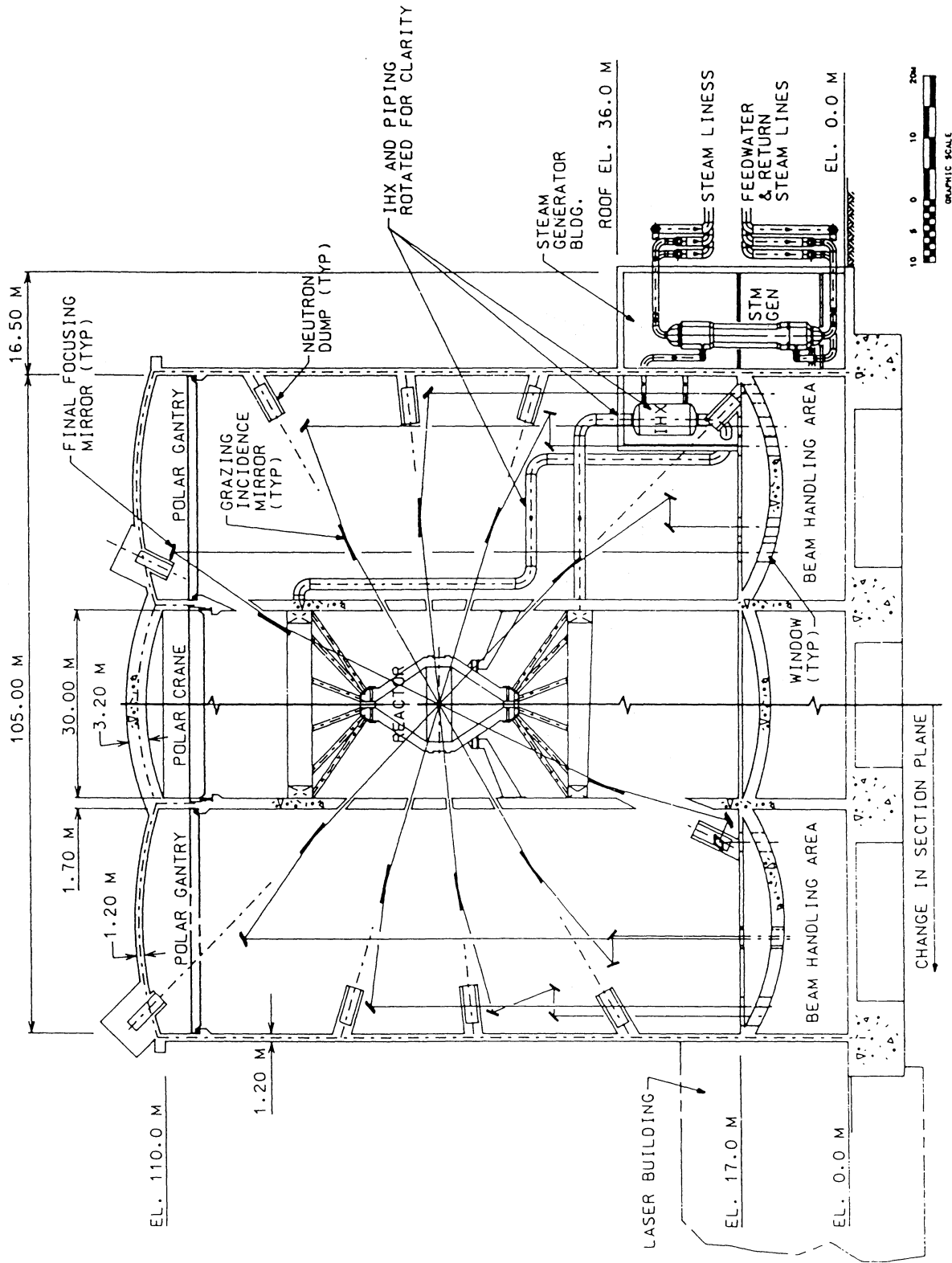


Fig. 3.3. Elevation view of the SOMBRERO reactor and steam generator buildings.

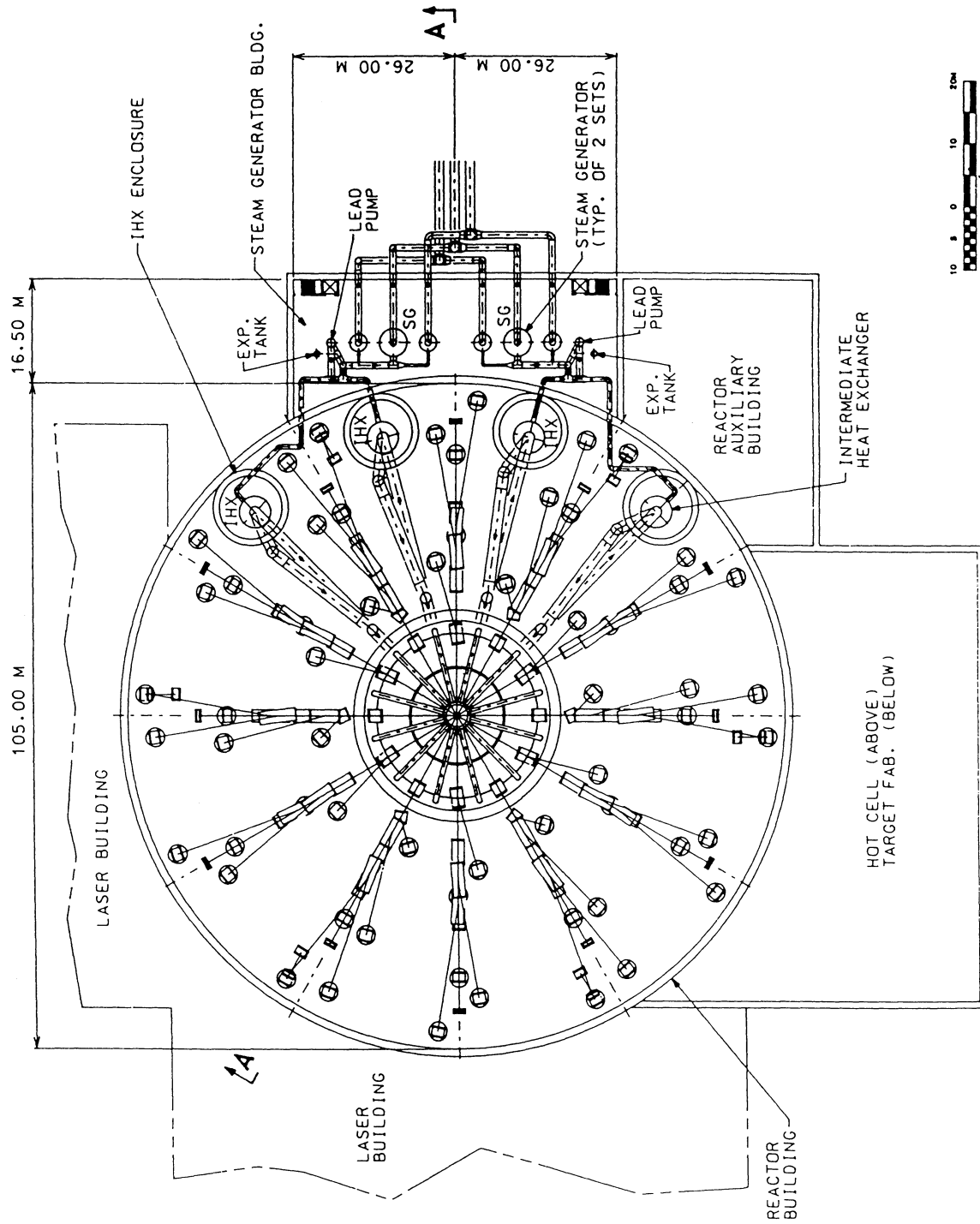


Fig. 3.4. Plan view of the SOMBRERO reactor and steam generator buildings.

replacement. In addition to the neutron dumps, the reactor building floor shields optics and equipment in the beam handling area.

Several unique features are incorporated in the reactor building structural concept. Since the building is required to operate in a vacuum, it is subject to an equivalent external pressure of about 0.1 MPa. For this reason, the floors and the ceilings are designed as shell structures rather than plates to reduce cost. The building has also been designed as a Seismic Category I structure and is adequately reinforced to resist buckling against external pressure.

A concept for the support of the grazing incidence and final focusing mirrors has been developed. As shown in Fig. 3.3, each mirror is separately supported. However, for structural rigidity, some of the supports are also tied together. Each support is a combination of reinforced concrete members. The supports are also configured so that the remote maintenance equipment can access the mirrors for replacement or refurbishment.

The IHXs are located within the reactor building. However, they are housed in individual cylindrical chambers. This arrangement accommodates the 0.1 MPa differential pressure (between the IHX chambers and the rest of the reactor building) and at the same time allows limited access to the IHX chambers during normal power operation. The steam generators are located in a separate building outside the reactor building.

3.4 KrF DRIVER DESIGN

3.4.1 Design Overview

There are several goals in the design of a KrF driver system for IFE: 1) high operating efficiency, 2) low capital cost, 3) technical credibility, 4) high availability / reliability, and 5) low operating costs. In this study we were to assume a tenth-of-a-kind plant with technology that could be mature in the year 2040. In creating a design, we focused on how to optimize operating efficiency.

A point design was carried out for a 3.6 MJ (on target) KrF laser. This is slightly higher than the 3.4 MJ we used as our reference design for the SOMBRERO power plant. To scale the design to the lower energy, the volume of the final amplifiers described in this section, would be reduced in proportion to the laser energy (i.e., by 5.6%). The design parameters for the 3.6 MJ point design are given in Table 3.3.

The KrF driver system consists of 1) a front-end which produces a pulse of the desired band width and temporal and spatial intensity characteristics, 2) several stages of intermediate amplification and progressive temporal/angular multiplexing, 3) final amplification by large e-beam pumped 2-pass amplifiers, and 4) demultiplexing and beam delivery to the reactor building. In the reactor building the beams are brought through a mirror system that provides neutron protection to

Table 3.3. KrF Driver and Amplifier Design Parameters

Overall Driver:	
Total Energy on Target (MJ)	3.6
Number of Beam Clusters	60
Beamlets per Cluster	100
Final Pulse Width (ns)	6
Efficiency (%)	7.5
Ultimate Amplifier:	
Final Amp Energy (kJ)	60
Ar in Kr (%)	50
Pressure (atm)	1
Initial Temperature (C)	500
Pumping (kW/cm ³)	400
Extraction Time (ns)	600
Amplifier Gain	16
Rep-Rate (Hz)	6.7
Length in Optical Direction (m)	1
Length in Flow Direction (m)	2
Length in E-beam Direction (m)	1
Flush Factor	1.3
Fluence (J/cm ²)	5
E-beam Voltage (kV)	610
Diode Current (A/cm ²)	40.6
Diode Impedance (ohms)	0.6
Inductance (nH)	23
Applied Field (kG)	6
Intrinsic Efficiency (%)	14.5

the laser stages and brings equal amounts of KrF illumination to the target from 60 uniformly-spaced directions by way of grazing incidence metal mirrors, which are the only optical element subjected to direct neutron flux. The ultimate amplifiers (UA's) in our system operate with a two-pass gain of 16, so the penultimate amplifiers (PA's) only supply ~6% of the total energy. From this, it is clear that the efficiency and the capital cost of the laser driver system are dominated by the UA's. Because of this, our design discussion at the conceptual stage focuses on consideration of

these amplifiers, how their efficiency may be optimized, and how they may most effectively be assembled into an architecture that satisfies the target requirements.

3.4.2 Key Features

We have produced a driver system design concept that is responsive to the requirements and goals listed above and has the following key features.

Direct Drive with Indirect Drive Brightness Capability. We have assumed the NRL, NIKE system approach for direct drive targets of "echelon-free ISI" in which a desired intensity profile is imaged onto the target through the laser chain, using partially coherent light. Broadband KrF emission with $\Delta\nu/\nu \sim 0.1\%$ is used to provide coherence times < 1 ps and thus allow rapid spatial averaging on the target. This approach utilizes imaging of a front end aperture through the whole amplifier chain, including angular multiplexing, to the target. It thus allows for the target beam spatial profile to change during the pulse and thereby takes advantage of the higher direct drive target gains that occur for a system that can zoom the target illumination spot as the target diameter decreases during irradiation. If new target designs favor indirect drive at a future date, we believe we could meet the requirements for indirect drive with a very similar system at similar cost. The ability of KrF driver systems to meet the brightness requirements for indirect as well as direct drive targets was described in a paper at the IAEA meeting on ICF Drivers in Osaka in 1991.¹²

E-Beam Pumping with High Efficiency. KrF laser kinetics and extraction physics have been studied in some detail since the first KrF lasing was achieved in 1975. Despite promising theoretical predictions for discharge and e-beam + discharge pumping, these approaches have not come close to the intrinsic efficiencies achieved by pure e-beam pumping ($\sim 14.5\%$ for our present design parameters). Low efficiency of the e-beam itself has been an area of concern for e-beam pumped systems; however, Textron has recently published a technology for e-beams that will allow them to operate at high average power, for long durations, and at high efficiencies - constrained only by the albedo of the laser gas mixture.¹³ E-beam efficiencies of $\eta_{eb} > 80\%$ are possible in the system we describe herein with 1 atm of 50% Ar + 50% Kr mixtures and titanium foils; η_{eb} approaching 90% should be possible with beryllium/aluminum foils. In these designs the e-beam is not allowed to intercept the foil support structure (i.e., the so called "hibachi" structure). The ability to achieve such "non-intercepting" operation has been experimentally demonstrated at Textron. This technology, coupled with the high voltage, cable-based pulse forming lines, a double foil system for removal of steady state waste heat, and the demonstrated high intrinsic efficiencies (14.5%) at high pump rate (400 kW/cm³) and high specific energy (30 J/l-atm for our design projections) for e-beam pumping, leads to an attractive design.

Angular Multiplexing for Pulse Compression. Pulse shortening from the many hundreds of nanoseconds required for efficient operation of large e-beam pumped amplifiers, to the ~ 6 ns required for target irradiation may be reliably and efficiently achieved, at reasonable system cost, by the use of angular multiplexing. Angular multiplexing shortens the beam pulse by using arrays of mirrors to direct different parts of the beam through different path lengths and then recombining the beam parts. By sending the later sections of the pulse through shorter path lengths, the pulse duration can be shortened to that of each beam section (e.g., breaking the beam into 100 sections will shorten the pulse length by a factor of 100). This has been developed for the Aurora (Los Alamos) and Nike (Naval Research Lab.) systems, as well as others at Rutherford in England, at the University of Alberta in Canada, and the Electrotechnical Laboratory in Japan. In some of these systems, angular multiplexing was used in concert with Raman beam combining. We have not utilized Raman technology because we believe we can achieve adequate beam quality from our amplifiers without the added cost and complication of Raman conversion.

Final Amplifier Total Efficiency Optimization and Waste Heat Utilization. High overall efficiency of the final or Ultimate Amplifiers is the key for achieving higher the driver system efficiency. Efficiency optimization requires consideration of the product of efficiencies resulting from consideration of charging the pulse forming lines, losses due to pulse rise and fall times, intrinsic efficiency, losses due to amplified spontaneous emission (ASE), power used for magnets for guiding the e-beams, flow power, fill factor for the angular cavity, and delivery of 60 beam clusters to the target. With our base case design, the laser efficiency is 7.5%. As previously noted, waste heat from the laser is used for feedwater preheat in the power conversion cycle, and this increases the plant thermal conversion efficiency from 45 to 47%. An equivalent view of benefit of using waste heat is an effective increase in the laser efficiency from 7.5% to about 9.5%.

3.4.3 Final Amplifier Design

We conclude that a good compromise can be achieved with a cavity of about 60 kJ capability (energy on target) with dimensions of 1 m × 2 m × 1 m for the e-beam direction, flow direction, and optical direction, respectively. Thus, the amplifier cavity window and mirror are each 1 m × 2 m (double pass), the e-beam area is 2 m × 1 m on each side (2-sided pumping), and the flow cross section area is 1 m × 1 m. The nominal amplifier specifications are given in Table 3.3.

Key elements of our technology choices include 1) the use of cable based pulse forming lines for high power flow capability (kW/cm^2), low cost, ease of maintenance, and flexibility in architecture, 2) use of a new, non-closing plasma cathode technology that allows the realization of non-intercepting e-beam design and, thus, albedo limited transport efficiency for e-beam power into the gas, 3) low inductance e-beam design using a race track bushing for low rise/fall times,

4) flow and acoustics design evolved from the DoD repped laser technology development of recent years, and 5) superconducting magnetic coil systems for the 6 kG applied fields required for e-beam guidance.

The amplifier pulse power system consists, in sequence to the e-beam, of a DC power supply, a modulator and energy storage system, switches, parallel pulse transformers, and a 1.25 MV charging line used to charge a set of parallel wired, paper-oil cables of the sort used currently for high voltage power transmission. The cables are ~30 cm diameter and ~60 m long (determined by the 600 ns pulse length desired and the dielectric constant of the oil/paper insulation). A laser-triggered rail gap output switch is used to transfer the energy from the set of cables to the e-beam diode, which has a 1 m × 2 m cathode. The use of parallel cables for the pulse forming line, as compared to water lines in single pulse test facilities, is an approach pioneered for use in high energy rep-rate lasers for DoD applications in recent years. The cables are a well-developed technology, have relatively low capital cost, are maintenance free, and because they are flexible, allow many possibilities in system architectures.

The flow system for one of the laser cavities requires a blower to move the gas at velocity of about 20 m/s and a heat exchanger to remove the waste heat (only ~12% of energy deposited in the gas comes out as photons; the rest goes to waste heat). There are also large volumes of acoustic suppression material to damp the ~2 atm pressure jump that occurs from the deposited energy (~300 J/liter). In addition, there are flow mixers and thermal equalizers associated with reconditioning the flow between pulses to achieve the low values of RMS density perturbations consistent with maintaining good beam quality in the amplified laser beam. A nominal design consistent with these requirements is shown in Fig. 3.5. From this, we see that a 2 m flow length cavity has given rise to a 30-m-long flow loop section. The required flow loop volume is dominated by the need to achieve acoustic suppression of the deposited energy, which is proportional to the energy required on target divided by laser efficiency. Minimizing flow loop volume is directly related to optimizing laser system efficiency.

We considered a number of ways of configuring the laser cavities and settled on the arrangement shown in Fig. 3.6. Fifteen of these flow loops, each with four cavities, will supply the nominal requirements of 3.6 MJ on target. We include sixteen flow loops in the architecture, which provides four spare amplifier cavities.

The cavities in Fig. 3.6 operate as two pass amplifiers. This figure shows a grouping of four mirrors at the center of the flow loop. There is one mirror for each cavity, each set at a 45° angle to the line of sight to its cavity window. The dimensions of each mirror are 1.4 × 2 m (1 × 2 m projected area at 45°), matching the beam dimensions at the cavity mirror. The individual beams (each 6 ns long) are largest at the cavity mirrors and decrease as they go to the feed arrays. The bundles of beams from/to the feed array require approximately constant cross sectional area.

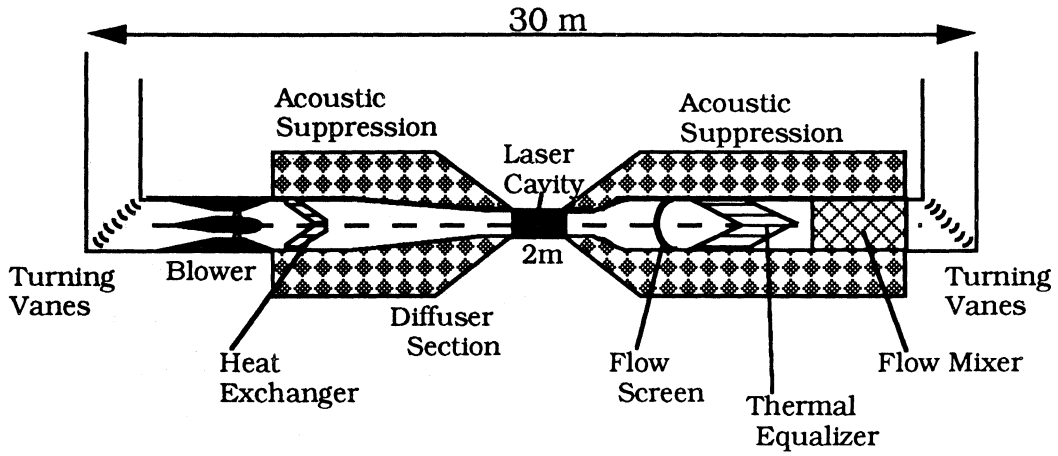


Fig. 3.5. Flow system for 60 kJ amplifier cavity (flow is from right to left).

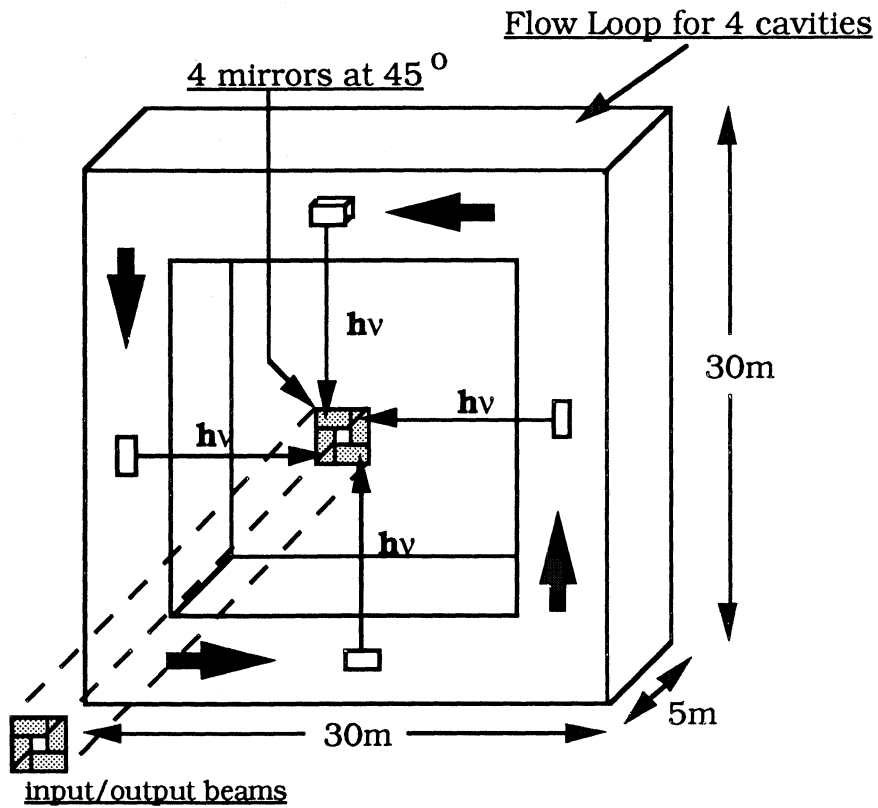


Fig. 3.6. Flow loop with four 60 kJ amplifier cavities.

Since the beam paths from the large amplifiers are in vacuum, there is an advantage in packing them together as they turn 90° to transmit from/to the feed arrays.

3.4.4 System Architecture

Our design is shown in Fig. 3.7. The total system is split into two equal parts located on the north and west sides, respectively (assume north at the top of the page). On the north side, we label the input/output array for the thirty-two 60 kJ amplifier cavities housed in eight flow loops.

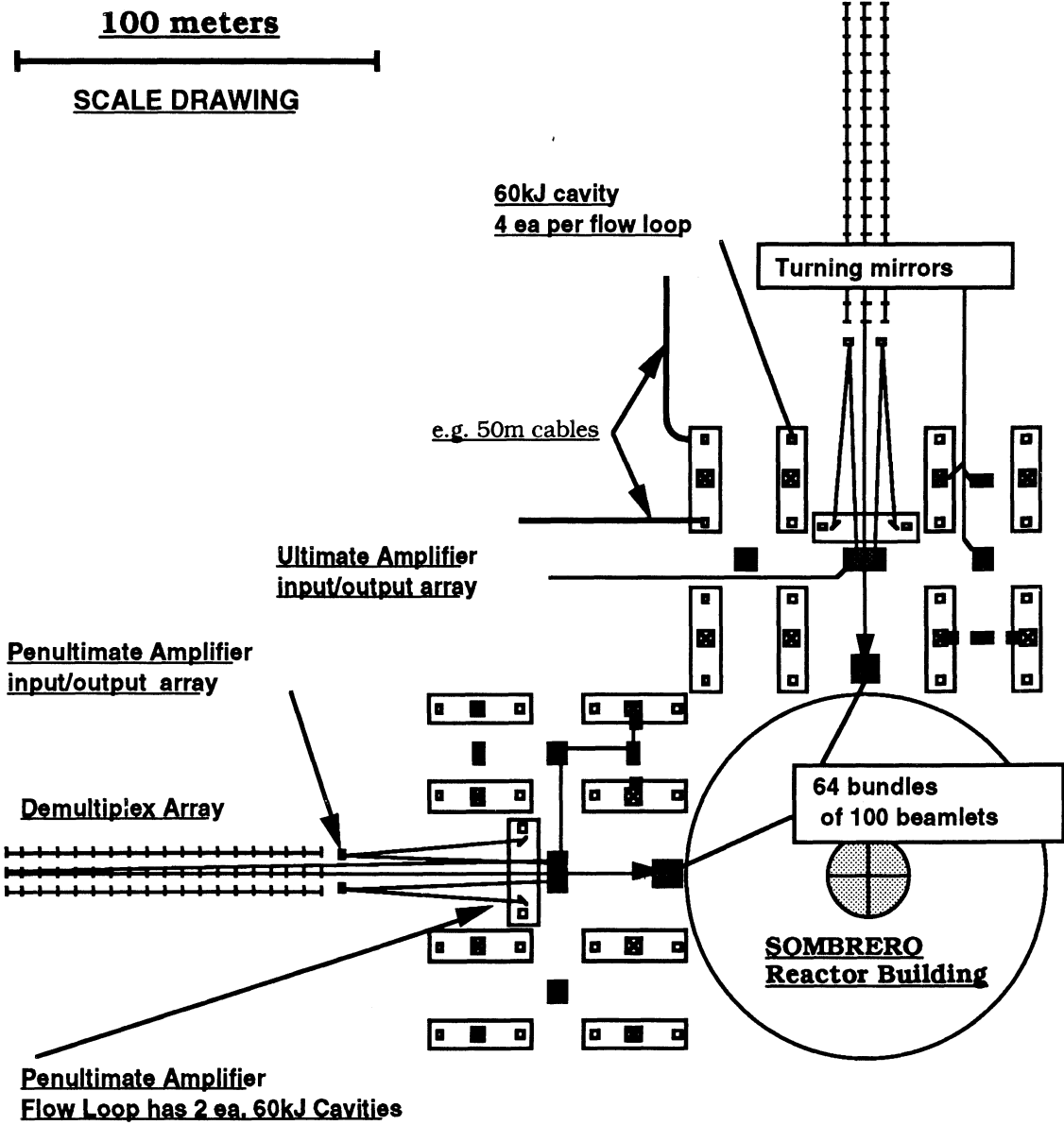


Fig. 3.7. Architecture for Ultimate and Penultimate amplifiers.

On the west side, we show a representative optical path of a single 6 ns beam leaving its 2×4 cm feed mirror, going north to a 45° turning flat, going east to the next 45° turning flat, then going north to the turning flat in the center of the flow loop, shown in Fig. 3.6, and then going into the appropriate one of the four 60 kJ cavities of this flow loop. One of these 6 ns pulses gets amplified to energy $\sim 60 \text{ kJ}/100 = 600 \text{ J}$ since we have multiplexed the 600 ns amplifiers to one hundred 6 ns beamlets. Thus, after a double pass transit of the amplifier the beamlet follows an angularly offset path back to the input/array where it is picked up on an 8×16 cm mirror which recollimates it and sends it west to the demultiplex array. The demultiplex array provides a designed time delay and then sends the beam on to the beam handling area under the SOMBRERO building.

The total number of 6 ns beamlets is $64 \times 100 = 6400$. 6000 of these are active at any time and are distributed into 60 directions onto the target. The directions are sorted in the beam handling area under the SOMBRERO building. If the beams go the most direct route possible, there are different path lengths to the target for each of the 60 directions. Appropriate time delays may be introduced via optical "trombones" in this area and/or by use of the demultiplex array trombones. Use of the extra four laser cavities, when needed, will require that they are able to supply any of the 60 directions, which will call for special trombones and mirror insertion possibilities in the design.

3.4.5 Conclusions

We have developed a KrF laser driver system design for power plant operation that has a 7.5% overall efficiency. We achieve this by having a carefully optimized overall laser system, by using high pump rate kinetics ($400 \text{ kW}/\text{cm}^3$) to achieve high intrinsic efficiencies (14.5%), by designing a low inductance diode structure, by using a break through gas/foil albedo limited, non-closing, non-intercepting e-beam, and by operating at high Joules/liter allowing efficient waste heat utilization. Our 60 kJ nominal size amplifier cavities give optimum efficiency and give an easy development size (the same cavity volume as the Large Aperture Module (LAM) of the Los Alamos Aurora system).

Finally, we believe our approach represents the best in low risk evolution from demonstrated technology. As in Aurora, we use e-beam pumping and angular multiplexing for pulse compression; as in Nike, we use Integrated Spatial Incoherence for smooth beam profiles in direct drive; and as in EMRLD, we use DoD-developed technology for repped excimer lasers of excellent beam quality.